

RSC Advances



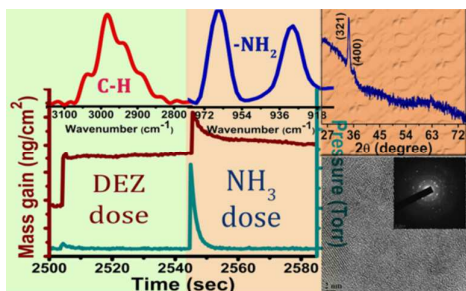
This is an *Accepted Manuscript*, which has been through the Royal Society of Chemistry peer review process and has been accepted for publication.

Accepted Manuscripts are published online shortly after acceptance, before technical editing, formatting and proof reading. Using this free service, authors can make their results available to the community, in citable form, before we publish the edited article. This *Accepted Manuscript* will be replaced by the edited, formatted and paginated article as soon as this is available.

You can find more information about *Accepted Manuscripts* in the [Information for Authors](#).

Please note that technical editing may introduce minor changes to the text and/or graphics, which may alter content. The journal's standard [Terms & Conditions](#) and the [Ethical guidelines](#) still apply. In no event shall the Royal Society of Chemistry be held responsible for any errors or omissions in this *Accepted Manuscript* or any consequences arising from the use of any information it contains.

TOC graphics:



Text:

Atomic layer deposition of crystallographically oriented and optically transparent Zn₃N₂ thin films deposited at 175-215°C.

Cite this: DOI: 10.1039/c0xx00000x

www.rsc.org/xxxxxx

ARTICLE TYPE

Atomic Layer Deposition of Textured Zinc Nitride Thin Films

Soumyadeep Sinha^a and Shaibal K Sarkar^{*a}

Received (in XXX, XXX) XthXXXXXXXXXX 20XX, Accepted Xth XXXXXXXXXXXX 20XX

DOI: 10.1039/b000000x

Zinc Nitride films are deposited by Atomic Layer Deposition (ALD) within a temperature range of 150°-315°C using Diethylzinc (DEZ) and Ammonia (NH₃). Self-limiting growth characteristics are examined by *in-situ* Quartz Crystal Microbalance (QCM) that is subsequently verified and complimented by *ex-situ* X-ray reflectivity (XRR) measurements. Saturated growth rate of ca. 1.4 Å per ALD cycle is obtained within the ALD temperature window of 175°-215°C. *In-situ* Fourier transformed infra-red (FTIR) spectroscopy is employed to study the reaction mechanism during each ALD half cycle. As deposited films on microscope glass substrates have strong orientation in {321} direction. Films are found transparent with high band-edge photoluminescence.

1. Introduction

Zinc Nitride is an n-type semiconductor with high electron mobility, carrier saturation velocity and large breakdown voltage. In recent time, its electrochemical properties as a cathode material in Li-ion battery were explored with reasonable success^{1,2}. Again oxygen incorporation in zinc nitride thin films, either in ambient or controlled condition, induces a rare p-type conductivity in (ZnO:N)^{3,4} that opens a vast new field of applications.

Several methods are used to deposit zinc nitride films, however MOCVD^{4,5} and reactive Sputtering^{6,7} are found to be the widely used techniques for Zn₃N₂ film deposition.

The ability to achieve conformal thin film with atomic level control of the film thickness makes Atomic Layer Deposition (ALD) a great tool in thin film deposition. It was initially introduced as Atomic Layer Epitaxy (ALE)^{8,9}, a modified version of CVD or MOCVD, where the reactants are fed to the reactor in a sequential manner. Its ability to obtain self-limiting surface reactions offers a good control over the stoichiometry, uniformity and step coverage.

ALD of metal nitrides are reported mostly with ammonia (NH₃) or hydrazine (N₂H₄) as the nitrogen source¹⁰. Considering the thermo-chemistry prospect, hydrazine could be a preferred nitrogen source than NH₃ but it is usually restricted due to safety issues. Diethylzinc (DEZ) is an established source of zinc that used to deposit ZnO^{11,12}. Use of metal-organics, in comparison to its halide salt, increases its volatility, thus enabling its easy carriage to the substrate. Also, often argued in literature that the organic part inhibit the film growth, enhance the reaction rate and dictates the morphology of the films¹³.

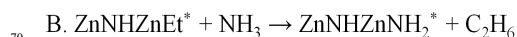
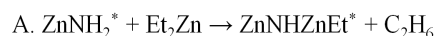
In this paper, we report ALD of oriented zinc nitride thin films on glass and Si (111) substrates using Diethylzinc (DEZ) and Ammonia (NH₃). Self-limiting growth mechanism was examined with *in-situ* QCM and *ex-situ* X-ray reflectivity (XRR) measurements. Under surface saturated regime the growth rate

was found ca. 1.4 Å per ALD cycle in the temperature window ranging from 175-215°C. The deposition chemistry was studied by *in-situ* FTIR spectroscopy and the elemental analysis of the as deposited films was carried out by X-ray photoelectron spectroscopy (XPS) and also by Secondary Ion-Mass spectroscopy (SIMS) measurement. Films are found transparent to visible spectra with a bandgap of 3.2 eV. A strong band-edge photoluminescence was observed at room temperature.

2. Experimental section

A hot wall viscous flow ALD reactor was used to deposit zinc nitride on microscopic glass and Si substrates. The description of the reactor was given elsewhere. Ultra high purity of N₂ gas was flown continuously (200 sccm) to keep the reactor base pressure constant at 1 torr that in turn also ensures a laminar flow inside the reactor. All the reactants were kept at room temperature and dosed into the reactor using N₂ carrier gas. The dose time was precisely maintained through computer-controlled pneumatic valves.

Following the trimethylaluminum (TMA)-NH₃ reaction^{14,15} to form aluminium nitride (AlN), proposed zinc nitride deposition chemistry was written in two separate surface limited half-reactions;



Where “*” denotes the surface species. Repeated AB cycles facilitate zinc nitride deposition.

During the zinc nitride deposition with repeated AB cycles, unless specified otherwise, the partial pressure of the DEZ (Sigma-Aldrich) and NH₃ exposure were kept invariably at ca. 0.1 and ca. 1.5 torr-s respectively. Throughout the course of film deposition, reactant exposure and purging time was maintained by time sequence m*t₁-t₂-n*t₃-t₄ where t₁ and t₃ are the dose time

for DEZ and NH_3 respectively while t_2 and t_4 are the purging time, which was customarily set for 40 sec. The dose time for DEZ and NH_3 were set for 1 sec, where m and n , the respective number of precursor exposures that was varied from 1 to 6. Reactant dosages were controlled by the use of pneumatic valves and mass flow controllers remotely controlled by a computer. The pressure change in the reactor was monitored by the capacitance manometer (Baratron, MKS instruments), that was heated to avoid chemical condensation.

Gold-coated AT-cut quartz crystals having 6 MHz resonance frequency were used for *in-situ* QCM studies. Measurements were carried out using Inficon SQM-160 thickness monitor. The crystals were mounted in a drawer and retainer assembly and sealed with non-conducting silver epoxy to prevent gas flow into the crystal chamber. An additional positive pressure of 0.1 Torr was applied inside the crystal drawer assembly by keeping constant flow of nitrogen gas. The deposited mass was measured from the change in the resonance frequency of the crystal using Sauerbrey equation^{16,17}.

Film thickness, material density and the crystallographic information were obtained by X-ray reflectivity (XRR) and the X-ray diffraction (XRD) measurements using Rigaku Smartlab X-ray diffractometer equipped with Cu-K α source. Experimentally obtained XRR data were fitted using GlobalFit fitting software to obtain the film properties.

In-situ Fourier transformed infra-red (FTIR) spectroscopy were performed to study the surface-bound chemical reactions during each ALD half cycles. All *in-situ* FTIR measurements were performed in a different reactor that was equally equipped with programmable gas feed and capacitance manometer. The IR beam passed through the reactor equipped with ZnSe window and recorded with liquid nitrogen cooled MCT detector. The deposition chamber was isolated from the spectrometer with the help of two pneumatic gate valves. FTIR spectra were recorded with Bruker Vertex 70 spectrophotometer. Each scan presented here is an average of 100 scans taken within 370 - 4000 cm^{-1} with a resolution of 4 cm^{-1} . KBr pallets were used as substrate that was centrally located in the IR beam path.

High-resolution field emission transmission electron microscopy (HR-TEM, JEOL-2100F) and selected area electron diffraction patterns were investigated to obtain microstructural information of the as deposited films. Films on glass substrates were scratched with a sharp razor blade. The materials was then dispersed in IPA and then fished on the TEM grid.

Field emission scanning electron microscopy (SEM) was carried out in ZEISS Ultra-55 Scanning Electron Microscope to investigate the surface morphology the deposited film. A film of 500 ALD cycles under saturated pulsing condition at 215°C was grown on Si substrate for this purpose.

X ray photoelectron spectroscopy (XPS) measurements were performed with Thermo VG Scientific photoelectron spectrometer (MultiLab) equipped with Al-K α source (1486.6 eV) to find the nature of the constituent element that was complimented by the TOF-SIMS measurements.

Secondary Ion-Mass spectroscopy (SIMS) measurements were performed to examine relative concentration of the different elements along the depth of the film. The Time of flight SIMS (TOF-SIMS) was acquired using a PHI TRIFT V nanoTOFTM

instrument from Φ ULVAC-Physical Electronics, Mn, USA. Pulsed Primary beam of 30KeV Au⁺ ion source was used to bombard the samples as used for high mass resolution spectroscopy. 7KV Cs ions were scanned in a raster size of 400micron x 400micron in a dual beam mode for sputtering. Alternately the Au and Cs ions were used to acquire data and sputter the top layer respectively. All the samples acquisition was done in positive SIMS while the depth was measured by Dektak XT from Bruker.

Room temperature Photoluminescence (PL) measurements were carried out in Jobin-Yvon iHR550 monochromator by using 40 mW Kimmon laser (HeCd; $\lambda = 325$ nm) source in the wavelength range of 350–700 nm at 325 nm excitation wavelength. The PL spectra were deconvoluted into multiple Gaussian peaks, using a non-linear curve fitting program. The transparency of the films was determined by the UV-Vis transmission spectra measurement for the similar film using PerkinEmer, LAMBDA UV/Vis/NIR and UV/Vis Spectrophotometers-950.

3. Results and Discussions

3. 1. ALD growth study of zinc nitride thin films

During the Zn_3N_2 deposition, the film growth was continuously monitored by *in-situ* QCM. Figure 1(a) shows a characteristic growth of zinc nitride films measured by the *in-situ* QCM at 175°C on ALD grown ZnO coated surface. It is noteworthy here that the QCM crystals were initially coated with 300 cycles (ca. 50 nm) of ALD grown ZnO before hand in the same reactor using DEZ and H_2O . This reduces *rms* roughness of the Au coating on quartz substrate and also provide similar starting surface for different experiments. As shown in the figure that during the course of zinc nitride film growth, two distinct growth regimes were visible; nonlinear mass change during first few cycles followed by a linear mass growth regime.

Beyond the nonlinear nucleation regime, the zinc nitride film deposition was found linearly dependent with the number of ALD cycles. Here the average mass change per cycle was ca. 13 ng/cm^2 corresponding to a growth rate of ca. 0.14 Å per ALD cycle. Figure 1(b) shows a couple of representative ALD cycles from the linear growth regime along with the dose sequence measured by the Baratron capacitance manometer. As represents earlier in equations A and B, it is clearly observed in the figure 1(b) that the DEZ exposure resulted in a considerable mass change of ca. 7.58 ng/cm^2 (Δm_1) while the NH_3 exposure resulted a mass change of ca. ~ 3 ng/cm^2 (Δm_2).

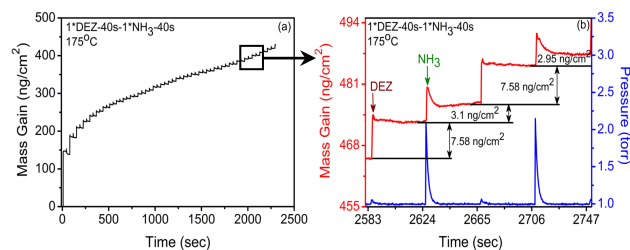


Fig. 1 (a) *In-situ*QCM growth characteristics of Zn_3N_2 ALD on ZnO coated gold crystal at 1*DEZ-40s -1* NH_3 -40s sequence of the precursors at 175°C. (b) QCM mass gain during two complete ALD cycles along with the precursor exposure at 175°C in the linear growth regime.

Thus the overall mass gain after one complete ALD cycle was found to be ca. 11 ng/cm² that contributes to the net growth of the material per cycle. Considering the mass density of zinc nitride 5.7 gm/cm³, determined by the XRR measurement, the net growth rate was found to be ca. 0.13 Å per cycle.

Furthermore, to validate the self-limiting growth mechanism, film deposition rate was measured with varied number of reactant dosages by *in-situ* QCM. The obtained growth rate was further verified with *ex-situ* XRR measurements. For XRR measurements, films were grown on Si wafers. All depositions were performed at 175°C. Figure 2(a) and (b) show the growth rate per ALD cycle with increasing number of reactant dosages that varied from 1 to 6 while keeping the dose time constant at 1 second.

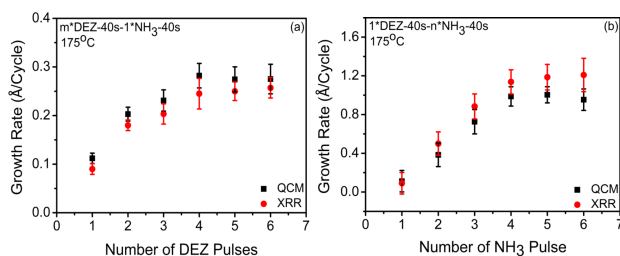


Fig. 2 Growth rate per cycle (Black: QCM and Red: XRR) as a function of number of (a) DEZ and (b) NH₃ exposure (Self-limiting characteristics) for the zinc nitride ALD at 175°C.

Thus, the reaction timing sequences can be written as m*1-40-1-40 and 1-40-n*1-40 for figure 2(a) and (b) respectively, where m and n is the number of pulses corresponding to DEZ and NH₃ exposure. It is clearly depicted from the figure 2(a) that 4 pulses of DEZ were required for a saturated growth rate of ca. 0.25 Å per cycle. A considerably high change in the growth rate was found with increase in ammonia (NH₃) dosages that saturates to a growth rate of ca. 1.1 Å per cycle. It is to be noticed that beyond this limiting value, inclusion of more reactants results no further increase in growth rate that invariably justified the self-limiting nature of zinc nitride ALD, a characteristics feature of the ALD growth mechanism.

3.2. Determination of Temperature window

We studied the growth rate per ALD cycle as a function of the deposition temperature to determine the ALD temperature window. The deposition rate was determined from the XRR measurements of the zinc nitride films on Si, deposited under saturated pulse condition.

Experimentally obtained Kiessing fringes were fitted with suitable model to obtain the thickness, density and roughness of the as deposited films. Figure 3 shows the average growth per cycle obtained for 300 cycles of zinc nitride films deposited on Si substrate at different substrate temperature. Inset shows a representative experimentally obtained Kiessing fringes along with the fitting for the film deposited at 195°C. It is depicted in the figure 3 where the average growth rate is nearly constant within the temperature range 150°-215°C. We defined this deposition temperature limit as the ALD temperature window. Increase in the deposition temperature results increase rate of desorption that results lowering the growth rate that is similar to the ones reported earlier^{17,18}

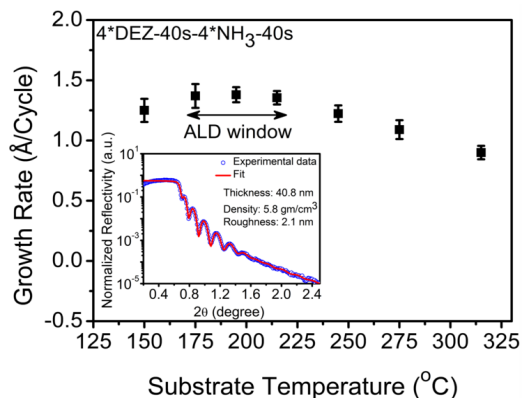


Fig. 3 ALD growth rate of Zinc nitride at saturated precursor exposure with the substrate temperature from 150°-315°C. (Inset) X-ray reflectivity measurement data and fitting of the film grown on Si substrate at 195°C.

3.3. In-situ FTIR spectroscopy studies of surface chemistry

The *in-situ* FTIR vibration spectroscopy was employed to determine the surface chemistry during each ALD half reaction. All study stated here are away from the nucleating regime that ensures no considerable effect of the substrate. Every spectrum was taken under the saturated dosage condition and at the end of every half cycle. The infrared difference spectra after each half cycle during zinc nitride growth are represented in figure 4. The difference spectra were obtained by considering the spectra of the previous half reaction as a reference. FTIR difference spectra, shown here, were taken after the 2nd and 3rd AB cycle of zinc nitride ALD after each sequential saturating exposure of DEZ and NH₃ respectively. In these difference absorbance spectra, the removal of surface species were indicated by the negative absorbance features while the positive absorbance features indicated the presence of the surface species.

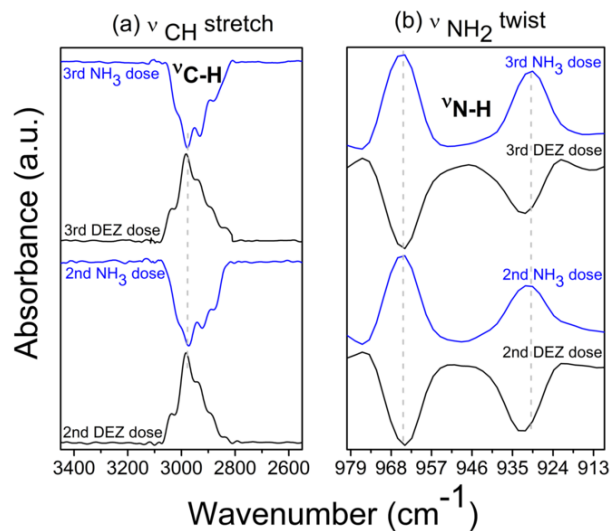


Fig. 4 *In-situ* FTIR difference spectra in the (a) C–H stretch and (b) –NH₂ twist regions after: 2nd and 3rd zinc nitride ALD cycles.

The FTIR spectra, as shown in figure 4(a), depicts the C–H stretching region^{12,19} from 2850 to 3050 cm⁻¹ that characterizes the appearance and loss of that particular surface species. The positive nature of the absorption peak corresponding to C–H stretch was observed after every saturated dose of DEZ. The clear

presence of C–H group after the DEZ dose indicated the presence of that particular adsorbed surface species during the 1st half reaction. Alternately the appearance of a symmetrical negative spectrum after every saturated dose of NH₃ indicated complete removal of the C–H group from the surface.

Thus the flip-flop appearances of the absorption peak corresponding to C–H stretch indeed proved the proposed surface half reactions as discussed earlier. Furthermore, complementary information could be found from the presence of –NH₂ surface species after the saturate NH₃ dosages.

The vibration spectra corresponding to –NH₂ twist¹⁰ appeared perfectly reciprocal to the C–H peak after every saturated dose of NH₃ at around 930 and 965 cm⁻¹ as shown in figure 4(b). Similar to the C–H stretch, here also the positive difference spectra indicated the appearance of the –NH₂ species while the negative spectra that appeared after the saturate DEZ dose proved the removal of the same surface species.

Thus the flip-flop appearance of the –NH₂ vibration peak during the ALD cycles were attributed to the other half ALD reactions. This indeed supplemented the information discussed earlier and hence completed a full ALD cycle.

3.4. Structural Characterization

Figure 5(a), (b) show X-ray diffraction pattern of zinc nitride films of thickness 70 nm taken under grazing angle incidence and Bragg-Brentano (θ - 2θ) configuration respectively. Films were deposited on glass substrates to avoid any crystallographic effect from the substrate.

It can be seen from figure 5(a) that the as deposited films show polycrystalline nature under the grazing angle configuration. Peaks at 31.7, 34.3, 36.6, 47.4, 56.5, 63 and 67.8 degree corresponding to the (222), (321), (400), (431), (600), (622) and (543) planes respectively of cubic zinc nitride (c-Zn₃N₂) matched with the JCPDS file (Card no. 00-035-0762).

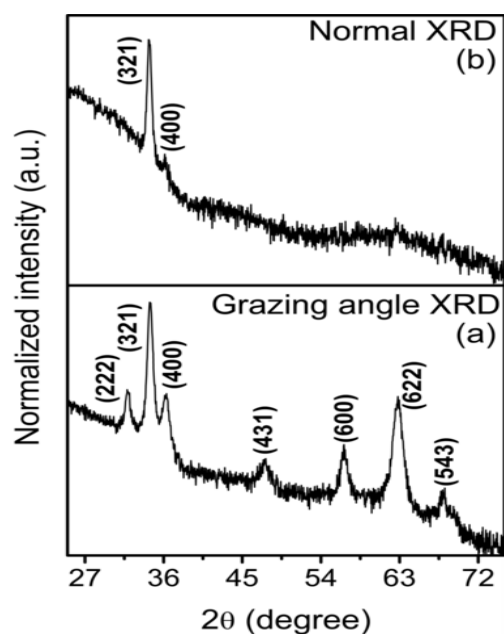


Fig. 5 X-ray diffraction patterns (a) grazing angle, (b) θ - 2θ of zinc nitride thin films deposited on glass substrate at 215°C substrate temperature.

The θ - 2θ measurements, as shown in the figure 5(b), basically

probe the orientation of the planes that are perpendicular to the substrates. A strong orientation along {321} direction is highly evident along with (400) from the θ - 2θ scan. Thus it can be concluded that the deposited film, though strongly oriented along {321} direction but indeed a polycrystalline film.

Figure 6(a) and (b) represents the HRTEM micrographs and the SAED pattern respectively of the as deposited films grown at 215°C. From the lattice imaging, measured interplanar spacing were found to be 0.262 nm, 0.286 nm, 0.19 nm and 0.208 nm that correspond to the (321), (222), (431) and (332) planes which incidentally matched with the peaks as found from XRD analysis.

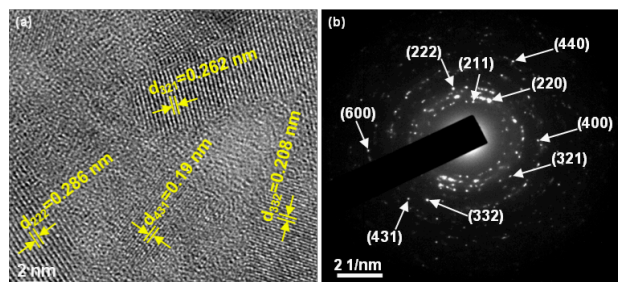


Fig. 6 (a) High Resolution Transmission Electron Microscopy image. (b) SAED patterns of zinc nitride film deposited on glass substrate.

Figure 6(b) shows the selected area electron diffraction (SAED) pattern where the diffraction rings represent the different planes of the crystal. From the SAED pattern, the interplanar distance of different planes such as (211) as 0.389 nm, (220) as 0.343 nm, (222) as 0.279 nm, (321) as 0.264 nm, (400) as 0.243 nm, (332) as 0.208 nm, (431) as 0.189 nm, (440) as 0.171 nm and (600) as 0.16 nm corresponds to the c-zinc nitride structure. Since the films were scratched out from a glass substrate there will be no effect from the substrate to the SAED pattern as well.

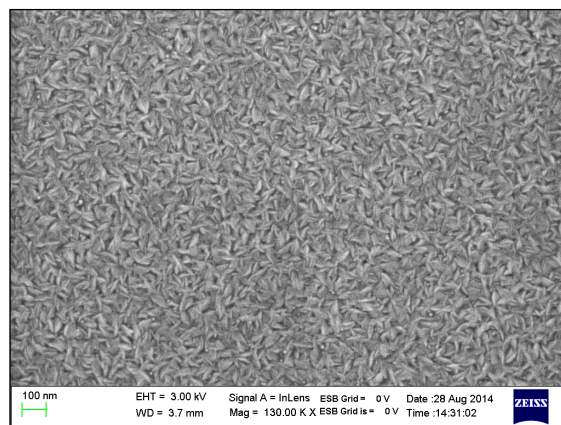


Fig. 7 Surface SEM image of the ALD grown zinc nitride film on Si substrate

Surface SEM image of the as-deposited Zn₃N₂ film grown on a Si substrate is shown in figure 7. A cross-hatched kind of surface morphology was observed in the grown film. The highly uniform film was also obvious as shown in the surface SEM image which further ensured the pinhole free deposition by ALD beyond doubt.

3.5. X-ray photoelectron spectroscopy (XPS) Study

The chemical nature of the as deposited material on Si substrate

was investigated by X-ray photoelectron spectroscopy (XPS). A wide scan of binding energy ranging from 0 to 1250 eV was measured to verify the presence of the constituents, as shown in the figure 8(a). The spectroscopy results presented here were taken after etching the film in Ar plasma for 3 min corresponding to a material removal of ca. 10 nm. A small but non-negligible appearance of the C 1s peak at 285.6 eV can be contributed from any incomplete reactions. As to be mentioned here that the film under test was grown under (1,1) pulse sequence of DEZ and NH₃ that is not under saturated growth regime. However, the atomic percentage of C was found to be under the experimental error limit.

It is a well attributed fact that zinc nitride is atmosphere sensitive and reacts with the moisture to form zinc hydroxide that further transformed to ZnO under suitable thermodynamic condition^{20,21}. The appearance of O 1s peak, as shown in the figure 8(b) thus represents an indication of room temperature degradation of zinc nitride film. The O 1s peak that appears consistently at 531 eV (among the several experiments we performed) can be attributed to the hydroxylated zinc nitride^{20,21} due to the limited air exposure and possibly not from the oxygen in ZnO. Here to be noted that the O 1s peak in zinc oxide appears at 530 eV²¹.

Figure 8(c) represents the Zn 2p_{3/2} peak at 1022.5 eV and Zn 2p_{1/2} peak at 1045.6 eV²² which are almost identical with the previous reports of Zn 2p peak of zinc nitride^{20,21}.

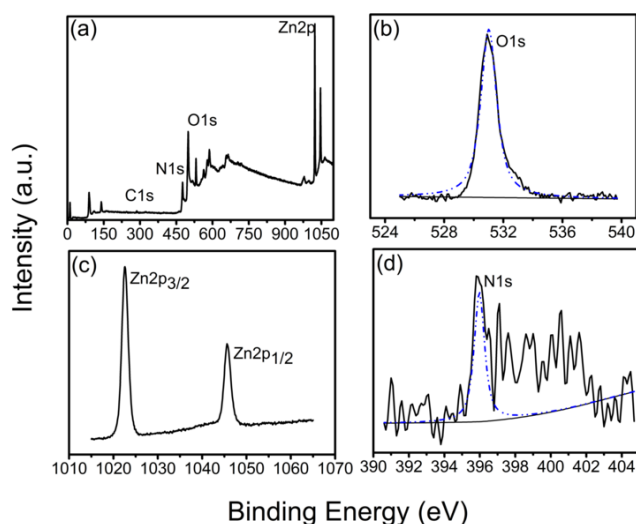


Fig. 8 X-ray photoelectron spectroscopy. (a) The typical XPS wide scan spectrum of ALD grown as deposited zinc nitride film on Si substrate, (b) O 1s peak, (c) Zn 2p peaks and (d) N 1s peak of zinc nitride.

The N 1s peak is shown in the figure 8(d). A relatively low intense N 1s peak at 396 eV corresponding to the main N 1s peak, (395.8 eV) indicates the N–Zn bonds^{20,21,22}. This relatively low intensity of the N 1s peak is also possible due to the denitrification during the Ar plasma etching, as reported by others^{7, 20, 22}. This refrain us from doing any further quantitative analysis from the XPS.

3.6. Secondary ion mass spectrometry (SIMS) measurement

Figure 9 shows the depth profile elemental analysis of the zinc nitride films deposited on Si substrate under saturated pulse condition and capped with ALD grown aluminum nitride (AlN) using Trimethylaluminum (TMA) and NH₃ as the ALD

precursors as reported earlier²³. Time of flight SIMS (TOF-SIMS) was used in static mode with Ga⁺ and Cs⁺ guns in a positive spectroscopy mode as sensitivity factor of metal species in negative mode is comparatively lower than that in positive mode. The TOF-SIMS profile represents the distribution of Zn, Al, O, N and C in the deposited stack of film and that of Si at the substrate.

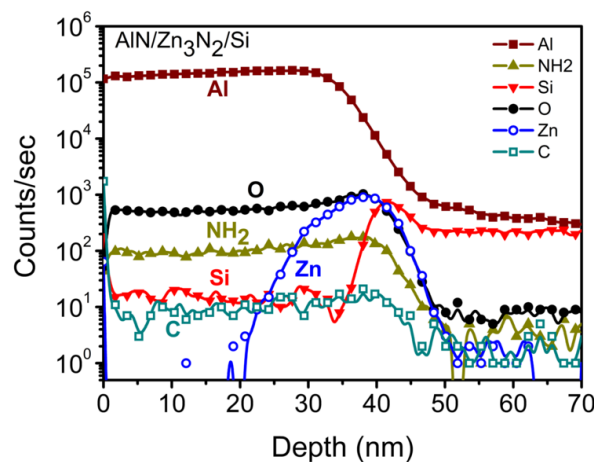


Fig. 9 Elemental analysis of the zinc nitride film by using TOF-SIMS depth profile which was deposited on Si substrate and capped with AlN.

The zinc nitride films used for characterization were capped with AlN thin films due to their high sensitivity towards atmospheric oxygen. The presence of this AlN layer at the top of stack is confirmed with high Al count at the beginning of profile. After sputtering 20-25 nm deep inside the sample depth, the concentration of Zn increases with simultaneous decrease in Al count and it goes down when the Si count increases at the interface of zinc nitride layer and Si substrate. Gradual decrease in Al concentration suggests the penetration of AlN in the zinc nitride film. The generated profile shows uniform distribution of NH₂ which proves the sufficient concentration of N in both nitride films. Molecular combination of NH₂ is considered in this case for the detection of Nitrogen ‘N’ as sensitivity of atomic N and its isotopes is low in positive mode while very close molecular weights of N₂ (28.01) and Si (28.08) makes it almost impossible to isolate between N₂ and ²⁸Si profiles. Figure 9 also suggests the presence of oxygen in the films which is also observed above in XPS analysis. The oxygen contamination can be primarily due to oxygen incorporation from oxidation of nitride films when exposed to ambient atmosphere^{20,21}. It was also reported earlier in case of ALE grown TiN films that nitride films get preferentially oxidized at the grain boundaries when exposed to ambient^{24,25}. Furthermore, it was noted that little C was present in the SIMS depth profile of the film stack. This attributes the absence of any unreacted organometallic species in the as deposited film. It is expected so as the film was grown under saturated dosages.

3.7. Optical measurement

The room temperature photoluminescence spectrum (PL) along with the UV-VIS transmission spectra of zinc nitride films deposited on quartz substrate are shown in figure 10. Except some interference loss at the film-substrate interface, it

was found to be transparent throughout the visible spectra. The bandgap of the film was found to be ca. 3.2 eV as determined from the Tauc plot, as shown in the inset.

The PL spectrum was measured with an excitation at 325 nm from a 40 mW laser source. A strong emission peak at 388 nm (~3.2 eV) was observed that corresponds to the band-edge recombination. Further analysis shows existence of sub-bandgap states that corresponds to the emission at ca. 420 nm (2.9eV) and at 530 nm (2.3 eV).

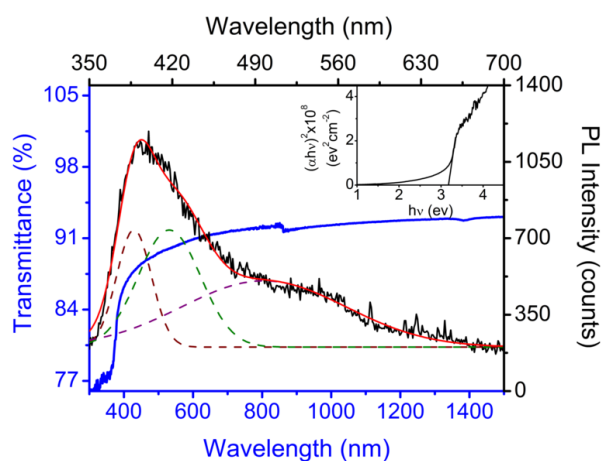


Fig.10 Transmittance spectrum (blue, solid) and the Photoluminescence (black, solid) spectrum of the ALD grown zinc nitride film on quartz substrate.

4. Conclusions

Here we demonstrated the deposition of zinc nitride films by sequential exposure of Diethylzinc (DEZ) and Ammonia (NH₃) within the ALD temperature window, 175°-215°C. Self-limiting behaviour of the ALD was verified by the *in-situ* QCM and *ex-situ* XRR measurements. The saturated growth rate ca. 1.4 Å per ALD cycle was observed within the thermal ALD window. Surface limited deposition chemistry was studied by *in-situ* FTIR vibration spectroscopy measurement. As deposited films on glass substrates were found polycrystalline but oriented along {321} direction. Room temperature photoluminescence show strong band-edge emission.

5. Acknowledgement

The authors thank the National Center for Photovoltaic Research and Education (NCPRE) aided by the Ministry of New and Renewable Energy, Govt. of India, for financial support. We thank Sophisticated Analytical Instrument Facility at IIT Bombay for materials characterization.

Notes and references

^a Department of Energy Science and Engineering, IIT Bombay, Mumbai-400076, India Fax+91 22 2576 4890; Tel: +91 22 2576 7846; E-mail: shaibal.sarkar@iitb.ac.in.

1. N. J. Dudney, *Mater Sci Engg: B*, 2005, **116**, 245.
2. J. B. Bates, N. J. Dudney, B. Neudecker, A. Ueda and C. D. Evans, *Solid State Ionics*, 2000, **135**, 33.

3. E. Kaminska, A. Piotrowska, J. Kossut, A. Barcz, R. Butkute, W. Dobrowolski, E. Dynowska, R. Jakiela, E. Przedziecka, R. Lukaszewicz, M. Aleszkiewicz, P. Wojnar and E. Kowalczyk, *Solid State Commun*, 2005, **135**, 11.
4. D. Wang, Y. C. Liu, R. Mu, J. Y. Zhang, Y. M. Lu, D. Z. Shen and X. W. Fan, *J. Phys.: Condens. Matter*, 2004, **16**, 4635.
5. E. Maile and R. A. Fischer, *Chem. Vap. Deposition*, 2005, **11**, 409.
6. F. Zong, H. Ma, W. Du, J. Ma, X. Zhang, H. Xiao, F. Ji and C. Xue, *Appl. Surf. Sci.*, 2006, **252**, 7983.
7. T. Yang, Z. Zhang, Y. Li, M. Lv, S. Song, Z. Wu, J. Yan and S. Han, *Appl. Surf. Sci.*, 2009, **255**, 3544.
8. S. M. George, *Chem. Rev.*, 2009, **110**, 111.
9. C. H. L. Goodman and M. V. Pessa, *J. Appl. Phys.*, 1986, **60**, R65.
10. B. B. Burton, A. R. Lavoie and S. M. George, *Journal of the Electrochemical Society*, 2008, **155**, D508.
11. J. W. Elam and S. M. George, *Chem. Mater.*, 2003, **15**, 1020.
12. J. D. Ferguson, A. W. Weimer and S. M. George, *J. Vac. Sci. Technol. A*, 2005, **23**, 118.
13. V. Miiikkulainen, M. Suvanto and T. A. Pakkanen, *Chem. Vap. Deposition*, 2008, **14**, 71.
14. H. Liu, D. C. Bertolet, J. W. Rogers and Jr., *Surf. Sci.*, 1994, **320**, 145.
15. R. L. Puurunen, M. Lindblad, A. Root and A. O. I. Krause, *Phys. Chem. Chem. Phys.*, 2001, **3**, 1093.
16. G. Sauerbrey, *Z. Phys.*, 1959, **155**, 206.
17. B. B. Burton, F. H. Fabreguette and S. M. George, *Thin Solid Films*, 2009, **517**, 5658.
18. S. K. Kim, C. S. Hwang, S.-H. K. Park and S. J. Yun, *Thin Solid Films*, 2005, **478**, 103.
19. D. N. Goldstein, J. A. McCormick and S. M. George, *J. Phys. Chem. C*, 2008, **112**, 19530.
20. M. Futsuhara, K. Yoshioka and O. Takai, *Thin Solid Films*, 1998, **322**, 274.
21. F. Zong, H. Ma, C. Xue, W. Du, X. Zhang, H. Xiao, J. Ma and F. Ji, *Mater. Lett.*, 2006, **60**, 905.
22. J. Nanke, G. G. Daniel, H. J. Ahalapitiya, W. C. Robert, C. Jie and M. Erik, *J. Phys. D: Appl. Phys.*, 2012, **45**, 135101.
23. X. Liu, S. Ramanathan, E. Lee and T. E. Seidel, *MRS Online Proceedings Library*, 2004, **811**.
24. M. Ritala, T. Asikainen, M. Leskelä, J. Jokinen, R. Lappalainen, M. Utriainen, L. Niinistö and E. Ristolainen, *Appl. Surf. Sci.*, 1997, **120**, 199.
25. M. Ritala, M. Leskelä, E. Rauhala and J. Jokinen, *J. Electrochem. Soc.*, 1998, **145**, 2914.